

Alaa Othman,^{1,2,3} Roberto Bianchi,⁴ Irina Alecu,^{1,2} Yu Wei,¹ Carla Porretta-Serapiglia,⁴ Raffaella Lombardi,⁴ Alessia Chiorazzi,⁵ Cristina Meregalli,⁵ Norberto Oggioni,⁵ Guido Cavaletti,⁵ Giuseppe Lauria,⁴ Arnold von Eckardstein,^{1,2,3} and Thorsten Hornemann^{1,2,3}



Lowering Plasma 1-Deoxysphingolipids Improves Neuropathy in Diabetic Rats



Diabetes 2015;64:1035–1045 | DOI: 10.2337/db14-1325

1-Deoxysphingolipids (1-deoxySLs) are atypical neurotoxic sphingolipids that are formed by the serine-palmitoyltransferase (SPT). Pathologically elevated 1-deoxySL concentrations cause hereditary sensory and autonomic neuropathy type 1 (HSAN1), an axonal neuropathy associated with several missense mutations in SPT. Oral L-serine supplementation suppressed the formation of 1-deoxySLs in patients with HSAN1 and preserved nerve function in an HSAN1 mouse model. Because 1-deoxySLs also are elevated in patients with type 2 diabetes mellitus, L-serine supplementation could also be a therapeutic option for diabetic neuropathy (DN). This was tested in diabetic STZ rats in a preventive and therapeutic treatment scheme. Diabetic rats showed significantly increased plasma 1-deoxySL concentrations, and L-serine supplementation lowered 1-deoxySL concentrations in both treatment schemes ($P < 0.0001$). L-serine had no significant effect on hyperglycemia, body weight, or food intake. Mechanical sensitivity was significantly improved in the preventive ($P < 0.01$) and therapeutic schemes ($P < 0.001$). Nerve conduction velocity (NCV) significantly improved in only the preventive group ($P < 0.05$). Overall NCV showed a highly significant ($P = 5.2E-12$) inverse correlation with plasma 1-deoxySL concentrations. In summary, our data support the hypothesis that 1-deoxySLs are involved in the pathology of DN and that an oral L-serine supplementation could be a novel therapeutic option for treating DN.

Diabetic neuropathy (DN) is one of the most important causes of morbidity and premature mortality in patients with diabetes (1,2). It generates a great economic burden through its complications, including foot ulcers caused by sensory loss and premature death caused by dysregulated autonomic functions (3,4). DN is a length-dependent axonal sensorimotor and autonomic neuropathy and usually starts in the lower extremities with either negative (e.g., numbness) or positive symptoms (e.g., neuropathic pain). Symptoms are mainly sensory and symmetrical on both sides, with a “stocking and gloves” distribution. Yet no adequate treatment for DN is available. Therapeutic options are restricted to treatment of symptomatic pain with costly medications and potential side effects.

The underlying pathomechanisms leading to DN are not yet understood. Several histopathological changes are associated with DN, including microangiopathy (5,6), direct nerve injury, and injury of the nerve supporting cells (e.g., Schwann cells in the peripheral nervous system or satellite cells in the dorsal root ganglia [DRG]). Hyperglycemia is considered an important contributor in the pathogenesis of DN (7–10), but even tight control of hyperglycemia is not sufficient to prevent DN (3,11–13). This suggests that other factors, in addition to hyperglycemia, underlie the pathogenesis of DN. Sphingolipids have been identified as emerging players in insulin resistance and type 2 diabetes mellitus (T2DM) (14). Sphingolipids are a heterogeneous class of lipids and essential components of the plasma membrane and plasma lipoproteins. The initial

¹Institute for Clinical Chemistry, University Hospital Zurich, Zurich, Switzerland

²Centre for Integrative Human Physiology, University of Zurich, Zurich, Switzerland

³Competence Centre for Systems Physiology and Metabolic Diseases, Zurich, Switzerland

⁴Neuroalgology and Headache Unit, IRCCS Foundation, Carlo Besta Neurological Institute, Milan, Italy

⁵Experimental Neurology Unit and Milan Center for Neuroscience, Department of Surgery and Translational Medicine, University of Milan-Bicocca, Milan, Italy

Corresponding author: Thorsten Hornemann, thorsten.hornemann@usz.ch.

Received 27 August 2014 and accepted 22 September 2014.

This article contains Supplementary Data online at <http://diabetes.diabetesjournals.org/lookup/suppl/doi:10.2337/db14-1325/-/DC1>.

A.O. and R.B. contributed equally to this study.

© 2015 by the American Diabetes Association. Readers may use this article as long as the work is properly cited, the use is educational and not for profit, and the work is not altered.

See accompanying article, p. 706.

and rate-determining step in de novo synthesis of sphingolipids is the condensation of palmitoyl-CoA and the amino acid L-serine—a reaction that is catalyzed by the enzyme serine-palmitoyltransferase (SPT) (15). Several missense mutations in SPT cause the hereditary sensory and autonomic neuropathy type 1 (HSAN1), a rare, length-dependent axonal neuropathy characterized by sensory loss, ulcers, and autonomic dysfunction (16,17). HSAN-1-causing mutations in SPT induce a gain of function by shifting the substrate affinity of the enzyme from L-serine to the noncanonical substrates L-alanine and glycine (18). This forms an atypical class of 1-deoxysphingolipids (1-deoxySLs), which lack the C₁-hydroxyl group of the canonical sphingolipids. Consequently, 1-deoxySLs cannot be metabolized to complex sphingolipids nor degraded by the canonical pathway, which requires the formation of sphingosine-1-phosphate as a catabolic intermediate. 1-DeoxySL concentrations are significantly elevated in the plasma of patients with HSAN1 as well as in the plasma and nerves of a transgenic HSAN1 mouse model (18,19). They are neurotoxic by inducing branching defects and neurite retraction in cultured primary DRG neurons (18). Interestingly, wild-type SPT is also able to metabolize L-alanine under certain metabolic conditions (20). We demonstrated in several clinical studies that 1-deoxySLs are significantly elevated in the plasma of individuals with metabolic syndrome and T2DM (21,22). Although the etiologies of HSAN1 and DN are different, the clinical presentation is rather similar. Both conditions are characterized by a painful, progressive, and length-dependent late-onset axonopathy that typically affects the distal extremities first. The degeneration of small intra-epidermal sensory fibers results in the loss of pain sensation, which in turn leads to painless injuries and neuropathic pain attacks. Both HSAN1 and DN are associated with painless skin ulcers and severely impaired wound healing, which is not typically seen in other peripheral neuropathies. We previously showed that oral L-serine supplementation significantly reduces the 1-deoxySL concentration in HSAN1 mouse models and patients (19). Moreover, L-serine-supplemented HSAN1 mice were protected from the development of neuropathy. On the basis of these findings, we were interested in whether L-serine is also effective in decreasing plasma 1-deoxySLs in the context of diabetes and whether such a treatment could be a therapeutic option for DN.

RESEARCH DESIGN AND METHODS

Animal Experiments

The Statement of Compliance (Assurance) with Standards for Humane Care and Use of Laboratory Animals was reviewed (28 October 2008) and approved by the National Institutes of Health Office for Protection from Research Risks (5023-01, expiration 31 October 2013). Male Sprague-Dawley rats (180–200 g; Charles River, Calco, Italy) were used for the study. The animals had access to food and water ad libitum. Diabetes was induced in

rats fasted overnight by a single intraperitoneal injection of 60 mg/kg streptozotocin (STZ) (Sigma, St. Louis, MO) dissolved in sodium citrate buffer (pH 4.5). Control rats were injected with only sodium citrate buffer (pH 4.5). Hyperglycemia was confirmed by measuring glycosuria 48 h after STZ injection (Keto-Diabur test; Roche Diagnostics, Spa, Italy). Blood glucose was determined after tail bleeding using the Ascensia Elite assay (Bayer, Basel, Switzerland). Food and water intake were assessed at the specified time points by averaging over a 2-day period. At the end of the study animals were killed; tissues were dissected and immediately frozen in liquid nitrogen.

Serine Supplementation

The animals had access to either a serine-enriched (containing 10% L-serine for the control group and 5% serine for the STZ group) or a standard diet (4RF21; Mucedola s.r.l, Milan, Italy). The serine content in the food for the STZ animals was halved to compensate for the doubled food intake of the STZ animals.

Behavioral Tests and Electrophysiology

Thermal and mechanical nociception were assessed as behavioral measures of DN. The nociceptive threshold to radiant heat was quantified using the hot-plate paw withdrawal test (23). In brief, a 40-cm-high Plexiglas cylinder was suspended over the hot plate, and the temperature was maintained at 50°C to give a latency period of approximately 10 s for control rats. Withdrawal latency was defined as the time between placing the rat on the hot plate and the time of withdrawal and licking the hind paw (or manifesting discomfort). Mechanical allodynia on the plantar surface of the rat was assessed by a dynamic paw withdrawal test with a Dynamic Plantar Aesthesiometer (Ugo Basile, Comerio, Italy), which generates a linearly increasing mechanical force. The paw withdrawal reflex was recorded automatically by measuring the latency until withdrawal in response to the applied force.

Nerve Conduction Velocity

Nerve conduction velocity (NCV) was measured as described previously (23). In brief, the antidromic sensory NCV in the tail nerve was assessed by placing recording ring electrodes in the distal tail. Stimulating ring electrodes were placed 5 and 10 cm proximally from the recording point. The latencies of the potentials, recorded at the two sites after nerve stimulation, were determined (peak to peak), and NCV was calculated. All of the neurophysiological parameters were determined under standard conditions and at a controlled temperature (room and animals). Core temperature was maintained at 37°C using heating pads and lamps.

Morphometric Analysis of the Caudal Nerve

The caudal nerve was fixed in 3% glutaraldehyde, post-fixed in osmium tetroxide, embedded in epoxy resin, and used for light microscopy and morphometric analysis. Semithin sections (1 μm) were prepared, stained with toluidine blue, and examined with a Nikon Coolscope light

microscope (Nikon Instruments, Calenzano, Italy). For the morphometric analysis, sections were analyzed using a photomicroscope (Nikon Eclipse E200; Leica Microsystems GmbH, Wetzlar, Germany) at a magnification $\times 60$, and the morphometric analysis was performed using a QWin automatic image analyzer (Leica Microsystems GmbH). All myelinated fibers in randomly selected sections from all specimens were counted, and the external (total) and internal (axonal) diameters of myelinated fibers were measured (at least 500 myelinated fibers/nerves). From both axonal and total fiber diameters, the histogram of fiber distribution was calculated and the ratio between the two diameters (g-ratio) was automatically calculated for each set of individual axon and fiber diameter. Histograms of the population distribution of myelinated fibers and axons, separated into class intervals increasing by 1.0 μm , were constructed.

Morphometric Analysis of DRG

At the end of the treatment period three L4-L5 DRG per animal were collected and postfixed in osmium tetroxide, embedded in epoxy resin, and used for light microscopy. For each animal, several semithin sections (1 μm) were prepared from randomly selected blocks and were stained with toluidine blue, then examined with a Nikon Coolscope light microscope (Nikon Instruments). The semithin sections were analyzed with a computer-assisted image analyzer (ImageJ software; National Institutes of Health, Bethesda, MD). The somatic, nuclear, and nucleolar sizes of DRG sensory neurons were measured for at least 200 DRG neurons/animal in randomly selected sections. All the morphometric measurements of caudal nerves and DRG were performed in a blinded fashion to which experimental group the specimen belonged.

Intraepidermal Nerve Fiber Density

Small-fiber peripheral nerve damage was assessed by quantifying the intraepidermal nerve fiber (IENF) density in the skin of the hind paw footpad (23). Hind paws were collected when the animals were killed, and 3-mm round samples of epidermis and dermis were taken by biopsy from the plantar glabrous skin and immediately fixed by immersion in 2% paraformaldehyde-lysine-periodate for 24 h at 4°C. Then the samples were cryoprotected overnight and serially cut with a cryostat to obtain 20- μm sections. Three sections from each sample were randomly selected and immunostained with rabbit polyclonal antiprotein gene product 9.5 antibodies (AbD Serotec, Kidlington, Oxfordshire, U.K.) using a free-floating protocol. The total number of polyclonal antiprotein gene product 9.5-positive IENFs were counted in each section under a light microscope at high magnification. Individual fibers were counted as they crossed the dermal-epidermal junction or were located in epidermal layer. Secondary branching within the epidermis was excluded. The length of the epidermis was measured using a computerized system (Image-Pro Plus; Media Cybernetics, Inc., Silver

Spring, MD), and the linear density of IENFs was obtained.

Na⁺/K⁺-ATPase Activity

Tibial stumps collected when the animals were killed were dissected, de-sheathed, and homogenized in chilled solution containing 0.25 mol/L sucrose, 1.25 mmol/L EGTA, and 10 mmol/L Tris (pH 7.5) at 1:20 (w/v). The samples were homogenized in a glass-glass Elvehjem-Potter (DISA, Milan, Italy) and stored at -80°C for ATPase determinations. Na⁺/K⁺-ATPase activity was determined spectrophotometrically, as described previously (23). Protein content in homogenates was determined using the Lowry protein assay with bovine serum albumin as the standard.

Sphingolipid Analysis

The sphingoid base composition of the extracted lipids was analyzed after hydrolysis, as described before (22). Isotope-labeled d7-sphingosine and d7-sphinganine (200 pmol; Avanti Polar Lipids, Alabaster, AL) was used as an internal standard. The sphingoid bases were separated on a C₁₈ column (120 Å, 5 μm , 125 \times 2 mm; Uptisphere; Interchim, Montluçon, France) and analyzed on a TSQ Quantum Ultra mass spec (Thermo, Reinach, Basel-Landschaft, Switzerland). Each sample was measured as a singleton. Intra- and interassay coefficient of variation (percentage) of the method was between 5 and 20%. The plasma and tissue concentrations of C₁₆SO, C₁₇SO, C₁₈SO, C₁₈SA, C₁₈SAdiene, C₁₈PhytoSO, C₂₀SO, C₂₀SA, and 1-deoxySA sphingoid bases were quantified.

Amino Acid Analysis

Amino acids were analyzed on a Zorbax Eclipse AAA column (150 \times 4.5mm, 5 μM ; Agilent) according to the manufacturer's instructions. A Shimadzu LC2010 high-performance liquid chromatography system connected to a fluorescence detector (Hewlett Packard) was used for detection.

Triglyceride Measurement

Triglycerides (TGs) were measured using an enzymatic assay kit (Sigma-Aldrich, St. Louis, MO) according to the manufacturer's protocol.

Statistical Analysis

Data are shown as mean \pm SEM. For normally distributed variables, one-way ANOVA was performed, followed by the Bonferroni correction for the multiple comparisons. In the Bonferroni correction, only four comparisons were considered: control rats on a standard diet versus control rats on a serine diet; control rats on a standard diet versus STZ rats on a standard diet; control rats on a serine diet versus STZ rats on a serine diet; and STZ rats on a standard diet versus STZ rats on a serine diet. Variables that were not normally distributed were log-transformed. Statistical analysis was performed using SPSS 16.0 (IBM, Zurich, Switzerland) and GraphPad Prism 5.04 (GraphPad Software, Inc., San Diego, CA).

RESULTS

Serine-Enriched Diet Increases Plasma Serine But Does Not Affect Body Weight, Hyperglycemia, Hypertriglyceridemia, or Food Intake in STZ Rats

An STZ-induced diabetic rat model was used to test the effect of oral L-serine supplementation on 1-deoxySL formation and DN. Two experimental designs were used (Fig. 1). In the preventive schedule, the animals had immediate access to either a serine-enriched or a standard diet. In the therapeutic schedule, animals remained on a standard diet for 8 weeks after STZ injection and then were randomized into groups receiving either a serine-enriched or a standard diet. STZ-treated animals developed hyperglycemia (Fig. 2A–C) within 48 h after injection. Hyperglycemia (400–800 mg/dL or 22.2–44.4 mmol/L) persisted in the STZ groups until the end of the study (preventive, 18 weeks; therapeutic, 24 weeks). Plasma TGs increased significantly in the diabetic animals, reaching a maximum after 4 weeks (300–400 mg/dL or 3.38–4.52 mmol/L), and remained elevated until the end of the study (Fig. 2D–F). Plasma serine concentrations were four- to sixfold higher in the serine-supplemented animals (Fig. 2G–I). This effect persisted until the end of the study. Serine supplementation did not affect hyperglycemia or hypertriglyceridemia (Fig. 2A–F) and had no influence on body weight or food or water consumption (Supplementary Fig. 1A–I). In contrast to controls the STZ group failed to gain body weight despite

the increased food and water intake (Supplementary Fig. 1A–C).

Serine-Enriched Diet Lowers 1-Deoxysphingolipids in the Plasma of STZ Rats Without Affecting Other Sphingolipids

Sphingoid bases in plasma are usually conjugated to a variety of *N*-linked fatty acids and different head groups. Because we were primarily interested in the sphingoid base profile, the *N*-acyls and head groups were removed by acid hydrolysis. The profile of the free sphingoid bases was analyzed using liquid chromatography–mass spectrometry. Consequently, the sphingoid base concentrations reported herein reflect the total concentrations of sphingolipids that are formed on a specific sphingoid base backbone.

Sphingolipids containing a C₁₈SO backbone were the dominant forms in plasma and did not differ between the groups (Fig. 3A–C). C₁₈SA concentrations were minor but increased initially in the serine-supplemented STZ animals, reaching a maximum after 3–4 weeks; then they decreased again but remained slightly elevated until the end of the study (Fig. 3D–F). C₁₈SA diene and C₁₈PhytoSO (Fig. 3G–L) were significantly elevated in all diabetic groups but did not change upon serine supplementation.

Plasma 1-deoxySA was significantly elevated in the STZ rats on a standard diet but remained low in the serine-supplemented STZ rats. In the preventive schedule, the plasma 1-deoxySA was significantly higher in the STZ

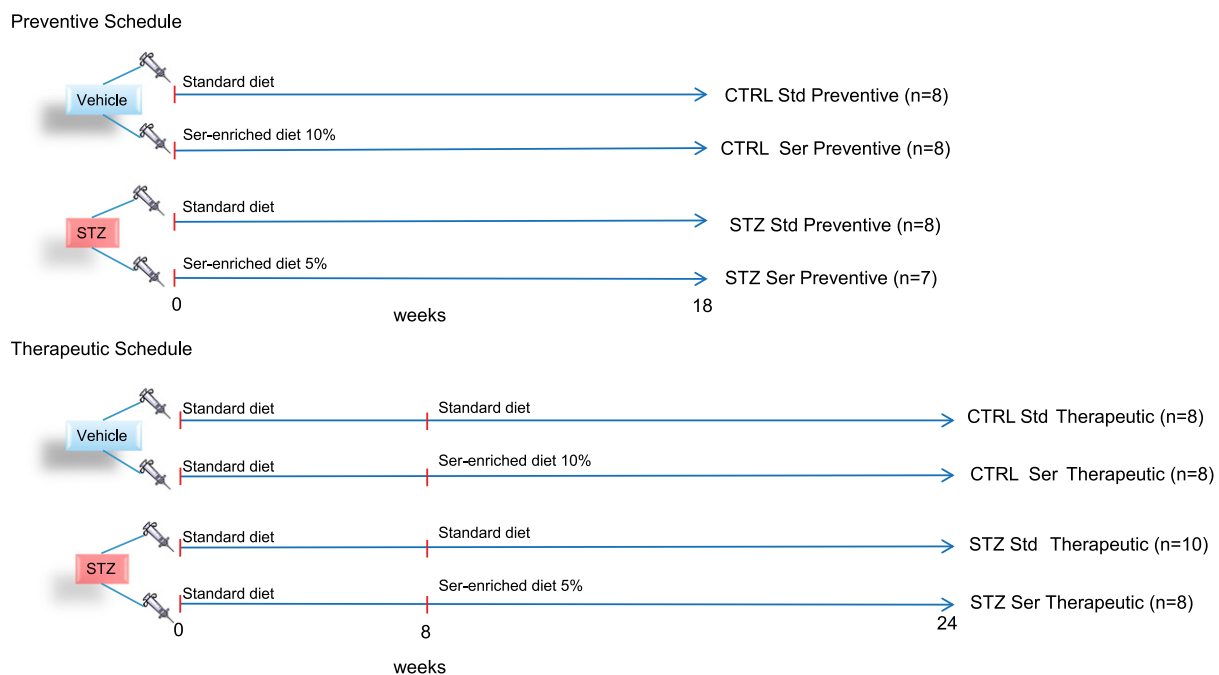


Figure 1—Schematic diagram showing the flow of the experiment. For the preventive schedule, a serine-enriched (Ser) or a standard diet (Std) was given from day 0 after STZ injection and the animals were followed for 18 weeks until they were killed. For the therapeutic schedule, animals received an initial standard diet for 8 weeks after STZ injection, followed by random separation into either a serine-enriched or a standard diet group. The animals then were followed until the end of the study period at week 24 after STZ.

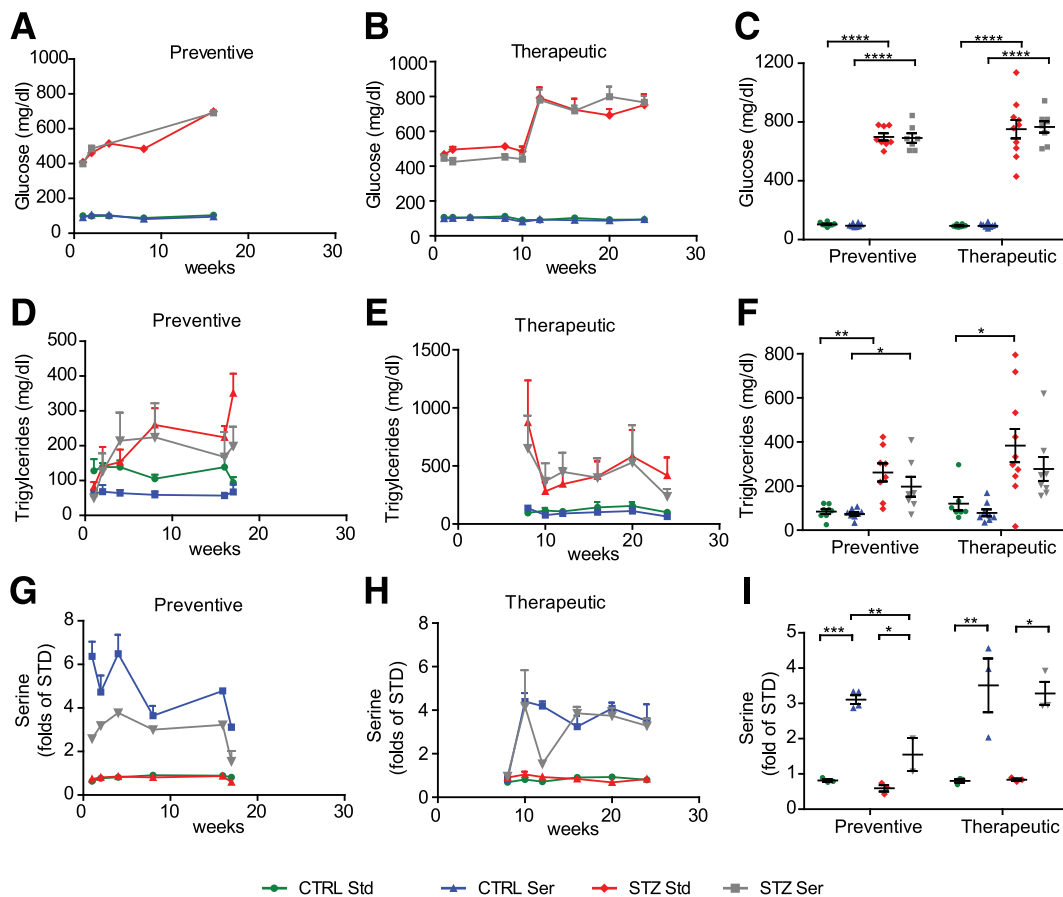


Figure 2—Effect of the serine-enriched diet on plasma concentrations of glucose, TGs, and serine. Line plots show the time course concentrations of plasma glucose (A and B), TGs (D and E), and serine (G and H) of the animals used in the study in the preventive (left) and therapeutic schedules (middle) for the different groups. Scatter plots show the values of plasma glucose (C), TGs (F), and serine (I) at week 16 after STZ injection for the preventive group and week 24 after STZ injection for the therapeutic group. The values are expressed as mean \pm SEM. *P* values were calculated using ANOVA followed by Bonferroni correction. **P* < 0.05, ***P* < 0.01, ****P* < 0.001, *****P* < 0.0001. CTRL Ser, control rats on serine diet; CTRL Std, control rats on standard diet; STZ Ser, STZ rats on serine diet; STZ Std, STZ rats on standard diet.

animals on a standard diet ($P < 0.0001$) compared with the other groups (Fig. 4A–C). 1-DeoxySA increased from $0.03 \pm 0.003 \mu\text{mol/L}$ at the beginning of the study to reach $0.05 \pm 0.007 \mu\text{mol/L}$ in the STZ rats on a standard diet before they were killed (Fig. 3A and C). The levels remained low in the serine-fed STZ rats until the end of the preventive scheme ($0.016 \pm 0.001 \mu\text{mol/L}$ at week 17 after STZ injection).

For the therapeutic scheme, we observed a rapid decrease of 1-deoxySA to control concentrations after switching to the serine-enriched diet in week 8, whereas 1-deoxySA concentrations remained high in the diabetic rats on a standard diet (Fig. 4B). This effect remained significant until the end of the study (Fig. 4B). No significant difference in 1-deoxySA concentrations was observed between the control rats with and without serine supplementation.

Plasma concentrations of $C_{16}\text{SO}$ (Supplementary Fig. 2A–C) did not differ significantly between the groups at baseline but were significantly reduced in the STZ groups

in both schemes at the end of the study. Plasma concentrations of $C_{17}\text{SO}$, $C_{20}\text{SO}$, and $C_{20}\text{SA}$ were not significantly different between groups and did not change upon treatment (Supplementary Fig. 2D–L).

Interestingly, we could not directly detect significant 1-deoxySA concentrations in nervous tissues, including the sciatic nerve, spinal cord, and DRG, of neither control or of diabetic animals (Supplementary Fig. 3). Overall distribution of sphingoid bases in the nervous tissues were similar between STZ and control animals. Compared with plasma, nervous tissue had a higher proportion of $C_{18}\text{SA}$ and $C_{17}\text{SO}$ and a lower proportion of $C_{18}\text{SAdiene}$.

Serine-Enriched Diet Improves the DN Phenotype in STZ Rats

STZ rats on a standard diet showed a significant decrease in the force withdrawal threshold, which was significantly improved in both groups supplemented with L-serine (Fig. 5A–C). In the preventive scheme, the force

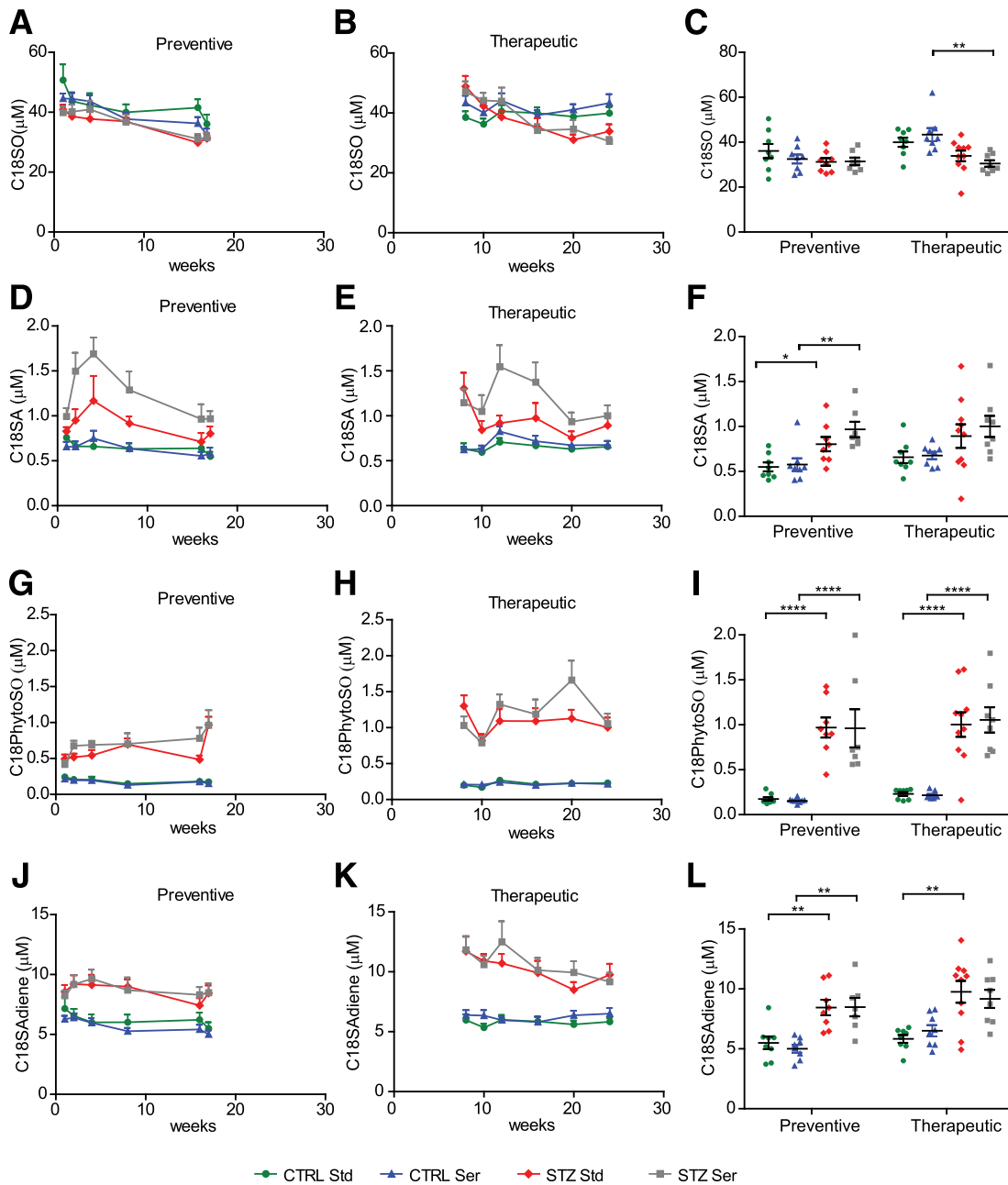


Figure 3—Effect of serine-enriched diet on plasma concentrations of typical sphingolipids. Line plots show the plasma concentrations of C₁₈SO (A and B), C₁₈SA (D and E), C₁₈PhytoSO-based sphingolipids (G and H), and C₁₈SAdiene (J and K) over the entire period of the preventive (left) and therapeutic schedules (middle) for the different groups. Scatter plots show the values for C₁₈SO (C), C₁₈SA (F), C₁₈PhytoSO (I), and C₁₈SAdiene (L) at week 17 after STZ for the preventive group and week 24 after STZ for the therapeutic groups. The values are expressed as mean \pm SEM. *P* values were calculated using ANOVA followed by Bonferroni correction. **P* < 0.05, ***P* < 0.01, *****P* < 0.0001. CTRL Ser, control rats on serine diet; CTRL Std, control rats on standard diet; STZ Ser, STZ rats on serine diet; STZ Std, STZ rats on standard diet.

withdrawal threshold remained stable for the serine-treated STZ animals (103.2 ± 11.6 g at week 14), whereas the STZ rats on a standard diet showed a continuous decrease over the whole study period (54.6 ± 5.0 g at week 14). A significantly improved mechanical sensitivity was observed for the serine-treated STZ rats versus those on a standard diet at the end of the preventive protocol (*P* < 0.01). No difference was seen between the

control groups. Similar results were obtained in the therapeutic scheme. Mechanical sensitivity was not significantly different between the STZ groups at the start of the serine supplementation at week 8 (74.5 ± 6.6 g in the STZ group on a standard diet and 73.4 ± 8.4 g in the STZ group on a serine-enriched diet). However, L-serine supplementation improved mechanical sensitivity, and the differences became significant at week 23 before the rats were killed

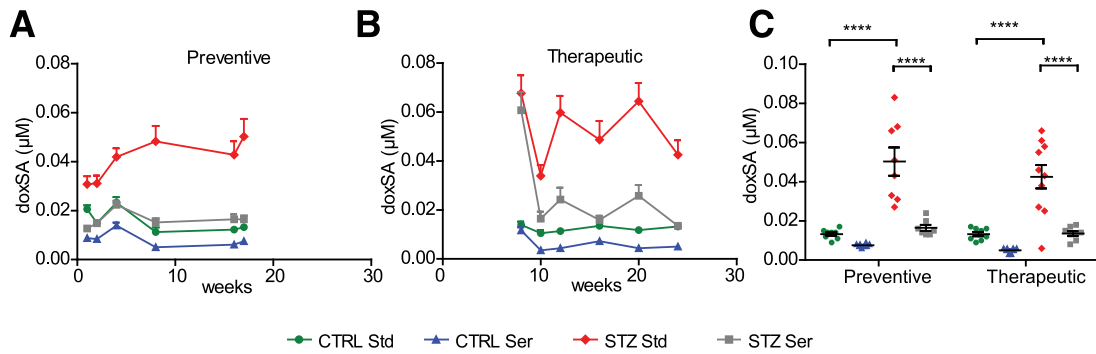


Figure 4—Effect of serine-enriched diet on plasma concentrations of 1-deoxySA. Line plots show plasma concentrations of 1-deoxySA (A and B) over the entire period of the preventive (left) and therapeutic schedules (middle) for the different groups. Scatter plots show the values for 1-deoxySA (C) at week 17 after STZ for the preventive group and week 24 after STZ for the therapeutic groups. The values are expressed as mean ± SEM. *P* values were calculated using ANOVA followed by Bonferroni correction. *****P* < 0.0001. CTRL Ser, control rats on serine diet; CTRL Std, control rats on standard diet; STZ Ser, STZ rats on serine diet; STZ Std, STZ rats on standard diet.

(52.0 ± 5.4 g on a standard diet and 101.8 ± 13.0 g on a serine-enriched diet; *P* < 0.001) (Fig. 5C).

Thermal response latency (Fig. 5D and E) was not significantly different between control and STZ animals in the preventive group but reached significance in the therapeutic group (Fig. 5F). L-serine supplementation showed no significant effect on thermal response latency.

NCV decreased significantly in the STZ groups on the standard diet (*P* < 0.0001 comparing the STZ-treated rats versus control rats on the standard diet in the preventive schedule; *P* < 0.001 comparing the same groups in the therapeutic schedule) (Fig. 6A). In the preventive scheme NCV was significantly improved in the STZ rats supplemented with L-serine (30.3 ± 2.2 m/sec in the STZ rats

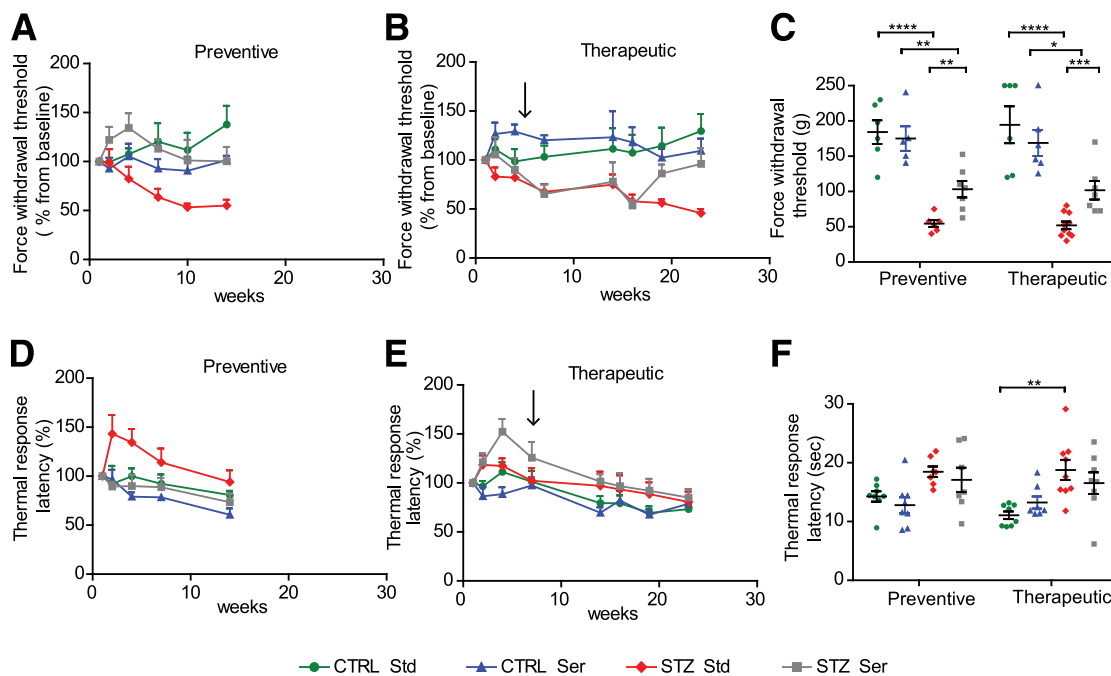


Figure 5—Effect of L-serine on of mechanical and thermal nociception. Force withdrawal threshold (A and B) and thermal response latency (D and E) were assessed for the preventive and the therapeutic groups at the beginning of the study and over time until the end of the study. Black arrows refer to the time when the serine-enriched diet was introduced to the respective groups in the therapeutic schedule. Scatter plots show the force withdrawal threshold (C) and thermal response latency (F) for the preventive groups at week 14 after STZ injection and week 23 after STZ injection for the therapeutic groups. The values are expressed as mean ± SEM. *P* values were calculated using ANOVA followed by Bonferroni correction. For the force withdrawal threshold, the values were log-transformed before the *P* values were calculated. **P* < 0.05, ***P* < 0.01, ****P* < 0.001, *****P* < 0.0001. CTRL Ser, control rats on serine diet; CTRL Std, control rats on standard diet; STZ Ser, STZ rats on serine diet; STZ Std, STZ rats on standard diet.

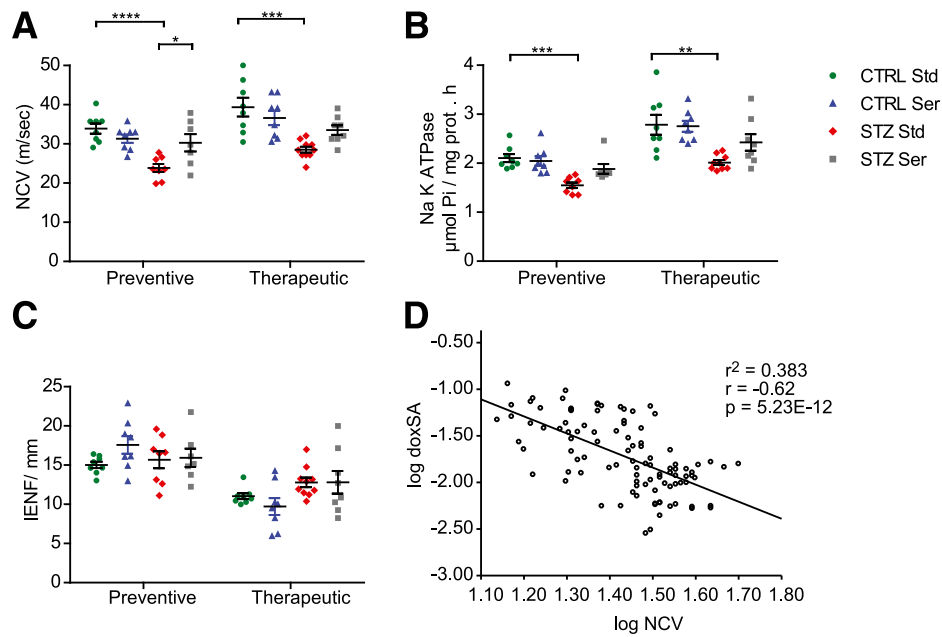


Figure 6—Effect of serine on sensory NCV (A), Na⁺/K⁺-ATPase activity (B), and IENF density (C). Scatter plots for the preventive (week 14 after STZ injection) and the therapeutic groups (week 23 after STZ injection). The values are expressed as mean \pm SEM. *P* values were calculated using ANOVA followed by Bonferroni correction. **P* < 0.05, ***P* < 0.01, ****P* < 0.001, *****P* < 0.0001. CTRL Std, control rats on standard diet; CTRL Ser, control rats on serine diet; STZ Std, STZ rats on standard diet; STZ Ser, STZ rats on serine diet. *D*: Scatter plot showing the correlation between NCV and plasma 1-deoxySA concentrations. A highly significant inverse correlation between plasma 1-deoxySA concentrations and NCV was observed of the whole group of animals (*P* = 5.23×10^{-12}). Variables were log-transformed because the control groups skewed the normal distribution to the right. Pearson correlation coefficient and the asymptomatic *P* value are shown.

on the serine-enriched diet vs. 23.8 ± 1.0 m/sec for the STZ rats on the standard diet; *P* < 0.05). By trend, NCV also improved in the therapeutic scheme but did not reach the statistical significance until the end of the study (Fig. 6A). Na⁺/K⁺-ATPase activity was significantly decreased in STZ rats on a standard diet in both the preventive and therapeutic groups (*P* < 0.001 and *P* < 0.01, respectively) (Fig. 6B). For both treatment schemes there was a trend for improved Na⁺/K⁺-ATPase activity upon serine supplementation, but this did not reach statistical significance after correcting for multiple comparisons. IENF density was not different between control and diabetic rats (Fig. 6C).

For all groups we observed a highly significant inverse correlation between plasma 1-deoxySA concentrations and NCV ($r = 0.62$; *P* = 5.23×10^{-12}) (Fig. 6D).

Nerve morphometry (Fig. 7A–D) indicated a change in the distribution of axon and nerve fiber diameters, with a smaller percentage of large-diameter fibers. This was partly restored upon L-serine supplementation in the preventive but not in the therapeutic group. In the preventive group the distribution of axon and nerve fiber diameters was significantly different in the L-serine-supplemented diabetic animals compared with those on a standard diet (*P* = 0.0001 for the distribution of axon diameter and *P* < 0.0001 for the distribution of nerve fiber diameter). This is mainly a result of the increase in the percentage of axons with a larger diameter (>7 μ m)

and a decrease in those with a smaller diameter (3–7 μ m). No significant difference in the distributions of axon/fiber diameter upon serine supplementation occurred for the therapeutic group. DRG neurons were smaller in the diabetic rats compared with controls and did not change upon supplementation (Fig. 8A). The morphometric analysis showed a significantly reduced somatic, nuclear, and nucleolar size in the DRG neurons of the diabetic animals compared with controls, independent of diet (Fig. 8C and D). No evidence of cell damage was observed, and satellite cells were normal in all groups.

DISCUSSION

We demonstrated previously that oral L-serine supplementation effectively lowers 1-deoxySL plasma concentrations in an HSAN1 animal model and patients with HSAN1 (19). Here we report that L-serine supplementation is also effective in reducing plasma 1-deoxySL concentrations in a diabetic STZ rat model. The reduced 1-deoxySL plasma concentrations were associated with improved sensory nerve function in the supplemented animals but had no effect on hyperglycemia or plasma TG concentrations (Fig. 2A–F). We found significant improvements in several neuropathy parameters, including mechanical sensitivity, NCV, the percentage of large-diameter fibers/axons, and, by trend, improved neuronal Na⁺/K⁺-ATPase activity. This indicates that lowering plasma 1-deoxySL concentrations is beneficial and

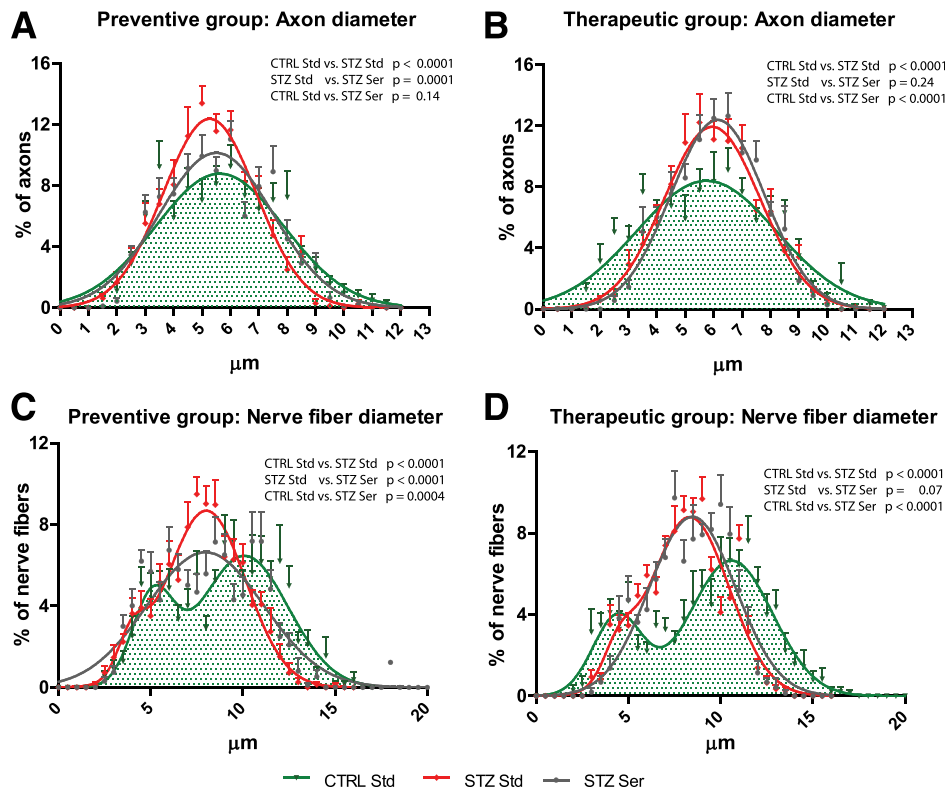


Figure 7—Effect of serine-enriched diet on axon, nerve fiber diameter. Distribution of axon (A and B) and nerve fiber diameters (C and D) shows a significant difference between the control and STZ rats (more axons and fibers with large diameters and fewer with shorter diameters in the control group). There is a significant improvement in the serine-supplemented STZ rats [STZ Ser] in the preventive group but not the therapeutic group (more axons and fibers with larger diameters and fewer with smaller diameters compared with the STZ rats on the standard diet [STZ Std]). Scatter plots show the mean \pm SEM for the frequency distribution of axons or nerve fibers (three replicates from each rat and three rats per group). The solid lines represent the fitted Gaussian distribution model. Nerve fiber diameter shows two Gaussian peaks in the control rats, denoting two different fiber types; this pattern is lost in the STZ rats. *P* values were calculated comparing the fitted Gaussian distribution of each group. CTRL Std, control rats on standard diet.

protects from diabetes-associated nerve damage. The negative influence of elevated plasma 1-deoxySL concentrations on nerve function is also supported by a highly significant negative overall correlation between plasma 1-deoxySLs and NCV.

STZ rats are generally considered to be a T1DM model; this notion is not, however, fully correct because hyperglycemia in these animals is typically also associated with early dyslipidemia and elevated plasma TGs (Fig. 2D–F). In patients with T1DM DN often develops after a period of sustained or uncontrolled hyperglycemia (24), which coincides with dyslipidemia in these patients (25). In patients with T2DM, dyslipidemia occurs early and even precedes the onset of hyperglycemia. Hypertriglyceridemia has been shown to correlate with the progression of DN independent of glycemic control (26,27). In the European Diabetes Prospective Complications Study (EURODIAB), hypertriglyceridemia was identified as an independent predictor of the development of DN in T1DM, even after adjusting for the duration of diabetes and HbA_{1c} (28). Plasma TG and 1-deoxySLs concentrations were shown to be independent variables but show a strong and highly significant correlation (21,22). This

correlation cannot be easily explained by direct metabolic interactions because 1-deoxySLs are formed by SPT through a shift of the amino acid, not of the lipid substrate. In contrast to TGs, whose concentrations in plasma are limited to millimoles, 1-deoxySLs are present in plasma and are neurotoxic *in vitro* at low micromolar values.

The mechanisms through which 1-deoxySLs exert their neurotoxic effects are not yet understood. They impair length, number, and branching of neurites in cultured DRG (18) and inhibit neurite growth and induced cytotoxicity in primary dopaminergic neurons (29). 1-DeoxySA can bind and activate endothelial differentiation gene (*EDG*) receptors in cell culture (30,31). The *EDG* receptor family consists of several G protein-coupled receptors that regulate various neuronal functions (32). Alternatively, 1-deoxySA may modulate protein kinase C activity; it was shown previously for other free sphingoid bases (33–35). Protein kinase C is involved in the pathogenesis of diabetic microvascular complications, including DN (36). Another line of evidence suggests that 1-deoxySLs impair neuronal cytoskeleton dynamics and growth cone formation (18). 1-DeoxySA promotes the disassembly of

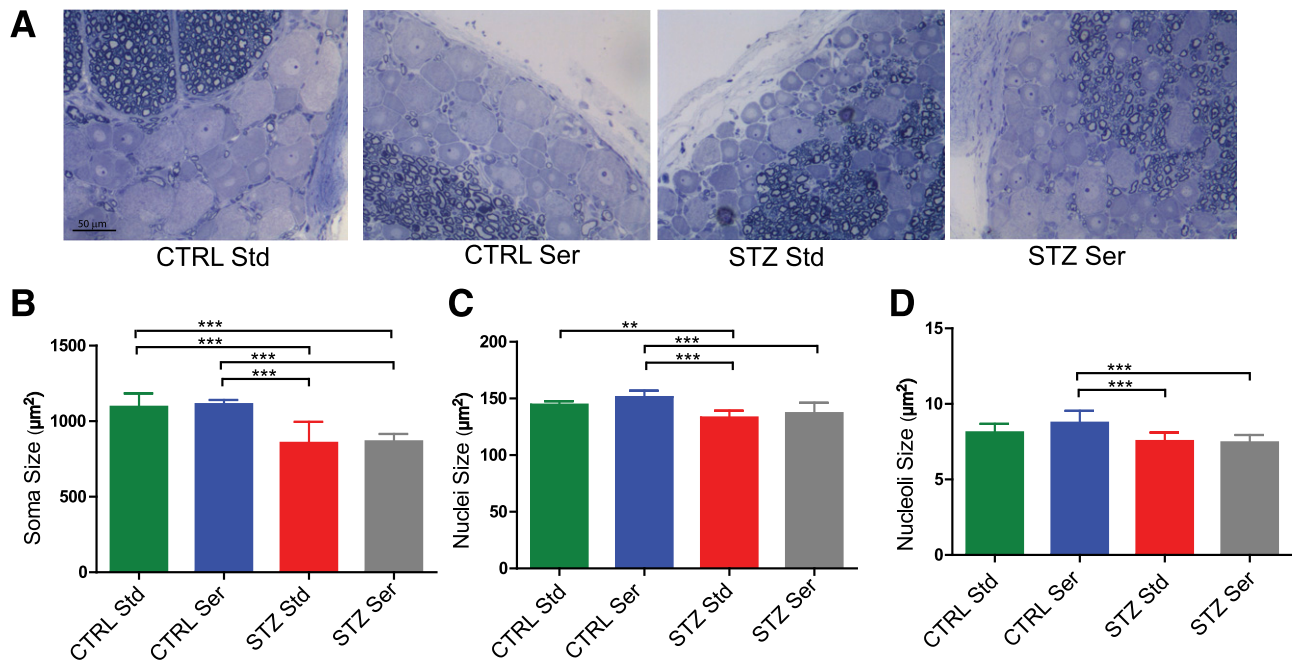


Figure 8—Effect of a serine-enriched diet on the morphometry of DRG neurons in the preventive group. *A*: Light microscopy of sections of DRG neurons in the preventive group stained with toluidine blue. DRG neurons of STZ-treated animals are smaller in size compared with control animals. No evidence of cell damage was observed. Column plots show the average size of soma (*B*), nuclei (*C*), and nucleoli (*D*) of DRG neurons in the control (CTRL) and STZ rats on a standard diet (Std) and a serine diet (Ser). The values are expressed as mean \pm SD. *P* values were calculated using ANOVA followed by the Tukey post hoc test. ***P* < 0.01, ****P* < 0.001.

actin stress fibers in Vero cells (37) and alters cytoskeleton dynamics in cultured INS-1 β -cells, resulting in the intracellular accumulation of filamentous actin, impaired insulin secretion, and the activation of Rac1 (38). However, we cannot fully exclude that the observed beneficial effects of L-serine are also mediated by other, not yet defined neurotropic mechanisms. Earlier reports showed that the addition of L-serine to embryonic chicken DRG improves neuronal differentiation and survival in vitro (39). Neurons cannot synthesize L-serine and therefore depend on the supply of serine from surrounding cells such as glia and satellite cells. Further mechanistic studies are therefore necessary to dissect the interplay between 1-deoxysphingolipid formation and the protective effect of serine in the context of DN. Independent of the underlying mechanisms, however, our studies unraveled oral L-serine supplementation as a candidate treatment for DN that merits further validation in clinical trials of patients with diabetes.

Funding. This work was financed by grants from the Gebert R uf Foundation; the Zurich Center of Integrated Human Physiology, University of Zurich (ZIHP); the 7th Framework Program of the European Commission (“RESOLVE,” project number 305707); and “radiz”—Rare Disease Initiative Zurich, University of Zurich.

Duality of Interest. No potential conflicts of interest relevant to this article were reported.

Author Contributions. A.O. designed the study, extracted lipids, analyzed mass spectrometry, quantified triglycerides, performed statistical analysis, and wrote the manuscript. R.B. and C.P.-S. designed the study and performed

the animal experiments, phenotyping, and neurobehavioral and neurophysiological tests. I.A. and Y.W. extracted lipids and homogenized tissue. C.P.-S., R.L., and A.C. conducted the experiments, including diet administration and blood sampling. C.M. performed behavioral tests. N.O. performed neurophysiological tests (nerve conduction velocity). G.C. and G.L. designed the study. A.v.E. designed the study, interpreted data, and critically revised the manuscript. T.H. performed the plasma serine measurements, designed the study, interpreted data, and supervised the study. T.H. is the guarantor of this work and, as such, had full access to all the data in the study and takes responsibility for the integrity of the data and the accuracy of the data analysis.

References

1. Dyck PJ, Kratz KM, Karnes JL, et al. The prevalence by staged severity of various types of diabetic neuropathy, retinopathy, and nephropathy in a population-based cohort: the Rochester Diabetic Neuropathy Study. *Neurology* 1993;43:817–824
2. Maser RE, Steenkiste AR, Dorman JS, et al. Epidemiological correlates of diabetic neuropathy. Report from Pittsburgh Epidemiology of Diabetes Complications Study. *Diabetes* 1989;38:1456–1461
3. Callaghan BC, Cheng HT, Stables CL, Smith AL, Feldman EL. Diabetic neuropathy: clinical manifestations and current treatments. *Lancet Neurol* 2012;11:521–534
4. Van Acker K, Bouhassira D, De Bacquer D, et al. Prevalence and impact on quality of life of peripheral neuropathy with or without neuropathic pain in type 1 and type 2 diabetic patients attending hospital outpatients clinics. *Diabetes Metab* 2009;35:206–213
5. Newrick PG, Wilson AJ, Jakubowski J, Boulton AJM, Ward JD. Sural nerve oxygen tension in diabetes. *Br Med J (Clin Res Ed)* 1986;293:1053–1054
6. Kennedy JM, Zochodne DW. Influence of experimental diabetes on the microcirculation of injured peripheral nerve: functional and morphological aspects. *Diabetes* 2002;51:2233–2240

7. Obrosova IG. Increased sorbitol pathway activity generates oxidative stress in tissue sites for diabetic complications. *Antioxid Redox Signal* 2005;7:1543–1552
8. Issad T, Kuo M. O-GlcNAc modification of transcription factors, glucose sensing and glucotoxicity. *Trends Endocrinol Metab* 2008;19:380–389
9. Vincent AM, McLean LL, Backus C, Feldman EL. Short-term hyperglycemia produces oxidative damage and apoptosis in neurons. *FASEB J* 2005;19:638–640
10. Vincent AM, Perrone L, Sullivan KA, et al. Receptor for advanced glycation end products activation injures primary sensory neurons via oxidative stress. *Endocrinology* 2007;148:548–558
11. The effect of intensive treatment of diabetes on the development and progression of long-term complications in insulin-dependent diabetes mellitus. The Diabetes Control and Complications Trial Research Group. *N Engl J Med* 1993;329:977–986
12. Duckworth W, Abraira C, Moritz T, et al.; VADT Investigators. Glucose control and vascular complications in veterans with type 2 diabetes. *N Engl J Med* 2009;360:129–139
13. Ismail BF, Craven T, Banerji MA, et al.; ACCORD Trial Group. Effect of intensive treatment of hyperglycaemia on microvascular outcomes in type 2 diabetes: an analysis of the ACCORD randomised trial. *Lancet* 2010;376:419–430
14. Hla T, Dannenberg AJ. Sphingolipid signaling in metabolic disorders. *Cell Metab* 2012;16:420–434
15. Hanada K. Serine palmitoyltransferase, a key enzyme of sphingolipid metabolism. *Biochim Biophys Acta* 2003;1632:16–30
16. Bejaoui K, Wu C, Scheffler MD, et al. SPTLC1 is mutated in hereditary sensory neuropathy, type 1. *Nat Genet* 2001;27:261–262
17. Roththier A, Baets J, Timmerman V, Janssens K. Mechanisms of disease in hereditary sensory and autonomic neuropathies. *Nat Rev Neurol* 2012;8:73–85
18. Penno A, Reilly MM, Houlden H, et al. Hereditary sensory neuropathy type 1 is caused by the accumulation of two neurotoxic sphingolipids. *J Biol Chem* 2010;285:11178–11187
19. Garofalo K, Penno A, Schmidt BP, et al. Oral L-serine supplementation reduces production of neurotoxic deoxysphingolipids in mice and humans with hereditary sensory autonomic neuropathy type 1. *J Clin Invest* 2011;121:4735–4745
20. Zitomer NC, Mitchell T, Voss KA, et al. Ceramide synthase inhibition by fumonisins B1 causes accumulation of 1-deoxysphinganine: a novel category of bioactive 1-deoxysphingoid bases and 1-deoxydihydroceramides biosynthesized by mammalian cell lines and animals. *J Biol Chem* 2009;284:4786–4795
21. Berteza M, Rützi MF, Othman A, et al. Deoxysphingoid bases as plasma markers in diabetes mellitus. *Lipids Health Dis* 2010;9:84
22. Othman A, Rützi MF, Ernst D, et al. Plasma deoxysphingolipids: a novel class of biomarkers for the metabolic syndrome? *Diabetologia* 2012;55:421–431
23. Bianchi R, Buyukakilli B, Brines M, et al. Erythropoietin both protects from and reverses experimental diabetic neuropathy. *Proc Natl Acad Sci U S A* 2004;101:823–828
24. Reh CMS, Mittelman SD, Wee CP, Shah AC, Kaufman FR, Wood JR. A longitudinal assessment of lipids in youth with type 1 diabetes. *Pediatr Diabetes* 2011;12:365–371
25. Young MJ, Boulton AJ, MacLeod AF, Williams DR, Sonksen PH. A multi-centre study of the prevalence of diabetic peripheral neuropathy in the United Kingdom hospital clinic population. *Diabetologia* 1993;36:150–154
26. Wiggin TD, Sullivan KA, Pop-Busui R, Amato A, Sima AA, Feldman EL. Elevated triglycerides correlate with progression of diabetic neuropathy. *Diabetes* 2009;58:1634–1640
27. Gordon Smith A, Robinson Singleton J. Idiopathic neuropathy, prediabetes and the metabolic syndrome. *J Neurol Sci* 2006;242:9–14
28. Tesfaye S, Chaturvedi N, Eaton SE, et al.; EURODIAB Prospective Complications Study Group. Vascular risk factors and diabetic neuropathy. *N Engl J Med* 2005;352:341–350
29. Martinez TN, Chen X, Bandyopadhyay S, Merrill AH, Tansey MG. Ceramide sphingolipid signaling mediates Tumor Necrosis Factor (TNF)-dependent toxicity via caspase signaling in dopaminergic neurons. *Mol Neurodegener* 2012;7:45
30. Salcedo M, Cuevas C, Alonso JL, et al. The marine sphingolipid-derived compound ES 285 triggers an atypical cell death pathway. *Apoptosis* 2007;12:395–409
31. Salcedo M, Cuevas C, Otero G, et al. The marine antitumor compound ES 285 activates EGD receptors. *Clin Cancer Res* 2003;9(Suppl.):6209s
32. Toman RE, Spiegel S. Lysophospholipid receptors in the nervous system. *Neurochem Res* 2002;27:619–627
33. Merrill AH Jr, Nimkar S, Menaldino D, et al. Structural requirements for long-chain (sphingoid) base inhibition of protein kinase C in vitro and for the cellular effects of these compounds. *Biochemistry* 1989;28:3138–3145
34. Merrill AH Jr, Stevens VL. Modulation of protein kinase C and diverse cell functions by sphingosine—a pharmacologically interesting compound linking sphingolipids and signal transduction. *Biochim Biophys Acta* 1989;1010:131–139
35. Hannun YA, Bell RM. Lysosphingolipids inhibit protein kinase C: implications for the sphingolipidoses. *Science* 1987;235:670–674
36. Geraldes P, King GL. Activation of protein kinase C isoforms and its impact on diabetic complications. *Circ Res* 2010;106:1319–1331
37. Cuadros R, Montejó de Garcini E, Wandosell F, Faircloth G, Fernández-Sousa JM, Avila J. The marine compound spisulosine, an inhibitor of cell proliferation, promotes the disassembly of actin stress fibers. *Cancer Lett* 2000;152:23–29
38. Zuellig RA, Hornemann T, Othman A, et al. Deoxysphingolipids, novel biomarkers for type 2 diabetes, are cytotoxic for insulin-producing cells. *Diabetes* 2014;63:1326–1339
39. Savoca R, Ziegler U, Sonderegger P. Effects of L-serine on neurons in vitro. *J Neurosci Methods* 1995;61:159–167